ELSEVIER

Journal of Nuclear Materials 266–269 (1999) 429–433

journal of nuclear materials

Molybdenum flux measurements in the FTU scrape off layer by deposition probes

M.L. Apicella [a,*], G. Maddaluno [a], V. Pericoli Ridolfini [a], R. Zagórski [b], C. Alessandrini [a], G. Apruzzese [a], G. Mazzitelli [a], D. Pacella [a], L. Verdini [a]

[a] *Associazione Euratom ENEA sulla Fusione, Centro Ricerche Frascati, C.P. 65, 00044 Frascati, Rome, Italy*
[b] *Institute of plasma Physics and Laser Microfusion, Warsaw, Poland*

Abstract

Space and time resolved measurements of the impurity particle fluxes in the scrape off layer (SOL) have been made on Frascati Tokamak Upgrade (FTU) by means of deposition probes. In this work experimental results are presented for ohmic plasma discharges with a molybdenum toroidal limiter, and with $B_T = 6$ T, $I_P = 0.7$ MA, $\bar{n}_e$ =(0.8–1.3) $\times 10^{20}$ m^{-3}. In the stationary phase the total collected molybdenum flux shows a large asymmetry between the electron and the ion side of the probes and the radial profiles are generally quite flat at low density. Simulations of the FTU SOL with the 2D multifluid numerical code EPIT reproduce the profile flatness only if a high perpendicular diffusion coefficient is assumed for the impurities. The code shows that the e^-/i^+ asymmetry can be accounted for by the shorter magnetic connection length on the e^- side (2.2 against 7 m).

Keywords: Collector probe; Edge plasmas; Molybdenum flux; 2D fluid code; Surface analysis

1. Introduction

High field compact devices as the Frascati Tokamak Upgrade (FTU) have employed materials with high atomic number Z as plasma facing components without any problem in their operations. This is due to the high density regimes of operations (line average density $\bar{n}_e$ up to 2×10^{20} m^{-3}) which result in a rather cool plasma edge and in a consequent low release of impurities.

A large database of FTU operations with medium and high Z materials, namely Inconel, Si, TZM(Mo), W, exists and their effects on the plasma are discussed in Ref. [1]. The main production mechanism for metallic impurities is physical sputtering by background ions and selfsputtering. Chemical sputtering is instead the cause for the release of light impurities as carbon and oxygen, which however are kept at very low level in the FTU plasma by means of a simple cleaning procedure (baking at 120°C and glow discharge in H_2).

To better investigate the impurity dynamics and the retention mechanism in the scrape off layer, deposition probes have been used recently for the first time on FTU. They are exposed in the plasma boundary and intercept charged particles flowing along magnetic field lines. The elements deposited in the upper layers of the probe material are analysed after extraction of the samples from the machine by using surface physics techniques.

In this paper we present and discuss the first results obtained in FTU with the sample introduction system to detect mainly molybdenum which is the material of the toroidal limiter. The system and the probe configuration are briefly described in Section 2. In Section 3 the experimental results for ohmic discharges are presented and discussed and compared with the predictions of a 2D transport code of the scrape off layer. In addition probe results are correlated with the molybdenum central density as measured by a rotating X-ray crystal spectrometer. In Section 4 the conclusions are drawn.

2. Experiment

The sample introduction system is composed of three subsystems: one for the introduction of samples into

* Corresponding author. E-mail: apicella@frascati.enea.it.

0022-3115/99/$ – see front matter
PII: S0022-3115(98)00536-4

FTU machine (Fig. 1); another for the storage and transportation of samples under vacuum from FTU to the surface analysis laboratory; the third one for the introduction of samples into the analysis chamber.

The sample is inserted in the vessel through a vertical port at $R = R_0$ where R_0 is the major radius of the vacuum chamber and at about 60° poloidally apart from the low edge of the toroidal limiter. The sample is supported by pneumatically operated pliers and can travel (1700 mm stroke) from a ten-samples stock to the plasma edge by means of the motor M2 and can be rotated by the sample rotation device driven by the motor M1. The distance of the top of the sample from the plasma centre can be varied across the SOL (Scrape Off Layer) between the limiter radius at $r = 29$ cm and the vacuum chamber wall at $r = 33.5$ cm.

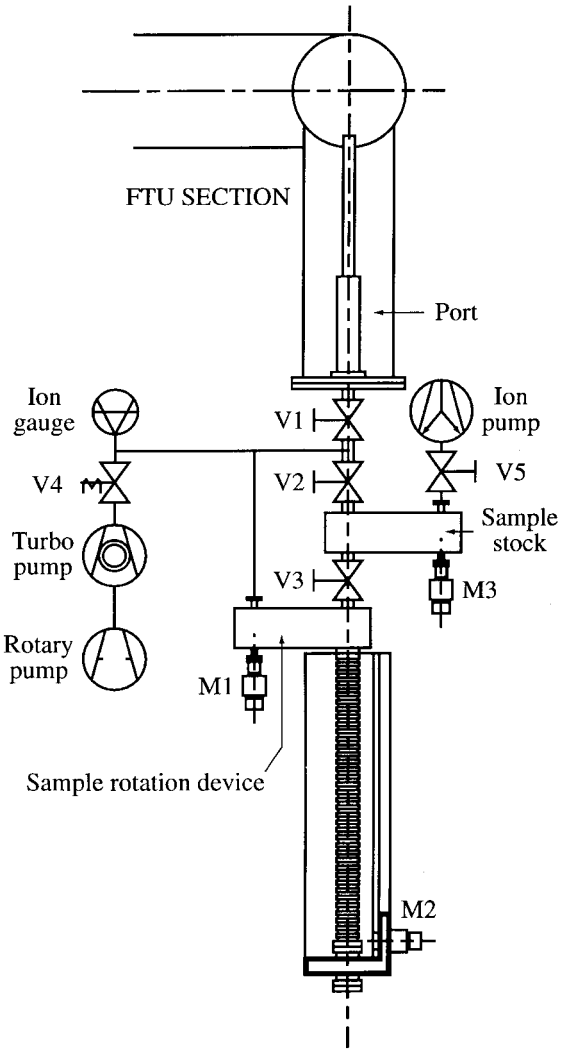

Fig. 1. Introduction subsystem diagram.

The probe is designed in order to get space and time resolved measurements of the particle fluxes (Fig. 2). It consists of a cylindrical graphite sample (diameter 25 mm) rotating inside a fixed titanium shield with two exposure slits (width 4 mm) placed on the electron and ion (e^-/i^+) side. Rotation is synchronised to the start of a given discharge and the time resolution is fixed by the ratio of the slit width to the rotation speed of the cylinder.

The width of the slits is greater than the gyro-radius ρ_i of impinging ions so that a reasonable transmission probability is expected. The worst case is for the Mo^+ ions having the largest $\rho_i = 1.3$ mm for $B_T = 6$ T and electron temperatures of 30 eV, typical of the FTU SOL. In this case a transmission factor of 45% at the slit centre is estimated assuming a Maxwellian velocity distribution [2] and it increases to 91% for the Mo^{++} ions. It must be pointed out that, according to the edge transport code EPIT [3], the contribution of the Mo^+ ions to the total flux of Mo is negligible at the probe location.

A reliable measurement of the absolute fluxes demands to reduce diffusion or evaporation of impurities on the probe. Graphite is a very good choice for its good thermal properties and for the high sticking coefficient of molybdenum which is very close to unity [4]. On the other hand, the probe itself is expected to perturb the plasma since it effectively acts as a limiter. Indeed the probe disturbing length [5] $L = d_h^2 c_s / D_\perp = 48$ m is larger than L_c, which is half the distance of the probe to the next obstacle, both for the ion side (7 m) and for the electron side (2.2 m). Here $d_h = 3$ cm is the lateral extension of the probe, c_s the ion acoustic speed ($= 5.4 \times 10^4$ m/s) and $D_\perp = 1$ m^2/s the perpendicular particle diffusion coefficient.

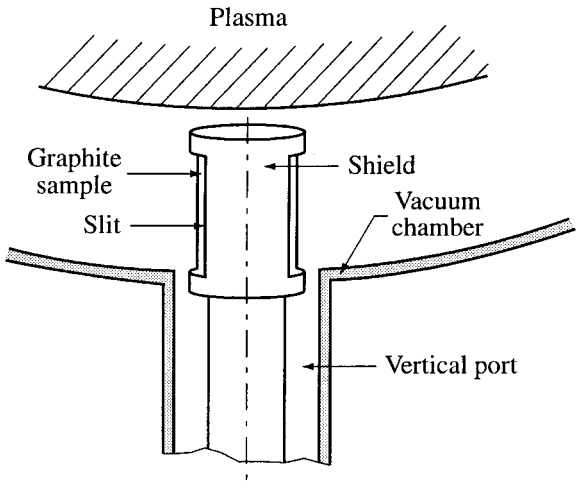

Fig. 2. Schematic view of the probe inside the vacuum chamber.

3. Results and discussion

In the present paper we describe the results obtained upon the exposure of the probes to ohmic plasma discharges, $B_T = 6$ T, $I_P = 0.7$ MA, $\bar{n}_e = (0.8–1.3) \times 10^{20}$ m^{-3}. This range of densities has been chosen because a considerable variation of Z_{eff} from 4 to 2 is obtained which is related to a reduction of metallic impurities produced at the limiter surface. The time resolution in all cases was of 0.16 s corresponding to the fastest rotation speed of 180° in 1.5 s of plasma duration. This choice has been made in order to reduce the damage to the probe material and to perform a more reliable quantitative analysis. In a few cases the probe was exposed to identical consecutive discharges to improve the signal to noise ratio of the measurements. After being exposed to the plasma discharge the probes were removed from the tokamak and the samples were analysed by the Auger technique to get the profile of the molybdenum concentration below the exposed surface. The depth resolution of the Auger technique is only a few angstroms and deeper regions of the sample were analysed by progressively removing the deposited material with an Ar ion beam. Measurements were performed at four different radial positions on four points along the lateral surface of the probe corresponding to the stationary phase of the discharge.

In Fig. 3(a) and (b) the molybdenum fluxes as a function of the plasma minor radius in the SOL at four different times are shown for a $\bar{n}_e = 0.8 \times 10^{20}$ m^{-3} plasma discharge for the i$^+$ and e$^-$ side, respectively. The radial profiles are quite flat, as also observed on other probes exposed to similar plasma conditions, and on the ion side it is about 3×10^{20} Mo atoms m^{-2} s^{-1}, 3.5 times larger than on the electron side. The scattering of the data must be attributed to the experimental error since no change in the plasma condition during the measurement time was observed.

Fig. 4 shows instead the same measurements for the i$^+$ side made at $\bar{n}_e = 1.3 \times 10^{20}$ m^{-3}. Close to the plasma the flux is lower than in the low $\bar{n}_e$ case by a factor of 3 and then radially decreases with an e-folding length <1 cm. On the electron side no measurements were possible because the signal was below the noise limit of the Auger technique.

The asymmetry at low density between the Mo fluxes onto the ion and the electron side agrees with the ratio (about a factor 3) of the two connection lengths defined by the probe and the toroidal limiter. This result agrees with the expectations that the impurity production is mainly proportional to the plasma flux onto the limiter. Indeed in a simple scrape-off model the parallel flux of plasma ions to the limiter balances the cross field flux from the central plasma which depends linearly on L_c: $\Gamma_\perp = D_\perp(n/\lambda)L_c w$. Here λ is the radial scale length of the density in the SOL and w is the poloidal extension of the probe.

To gain more quantitative information, the impurity transport inside the SOL has been investigated with a 2D multifluid code EPIT already used in the past to analyse the FTU data [3] and the results have been compared with the experiment. Two cases at low and high density have been considered, for either the ion and electron connections lengths (7 and 2.2 m, respectively). The code assumes that the probe acts as a limiter thus perturbing the plasma temperature and density inside the magnetic flux tube connected to the probe. The main input data for the code are: power input into the SOL: $P_{SOL} = (500, 600)$ kW, electron and ion heat perpendicular coefficient: $\chi_{e\perp} = 4$ m^2/s, $\chi_{i\perp} = 0.4$ m^2/s, electron, ion and impurity perpendicular diffusion coefficient: $D_{e\perp}$, $D_{i\perp} = 1$ m^2/s, $D_{imp,\perp} = (1,4)$ m^2/s depending on

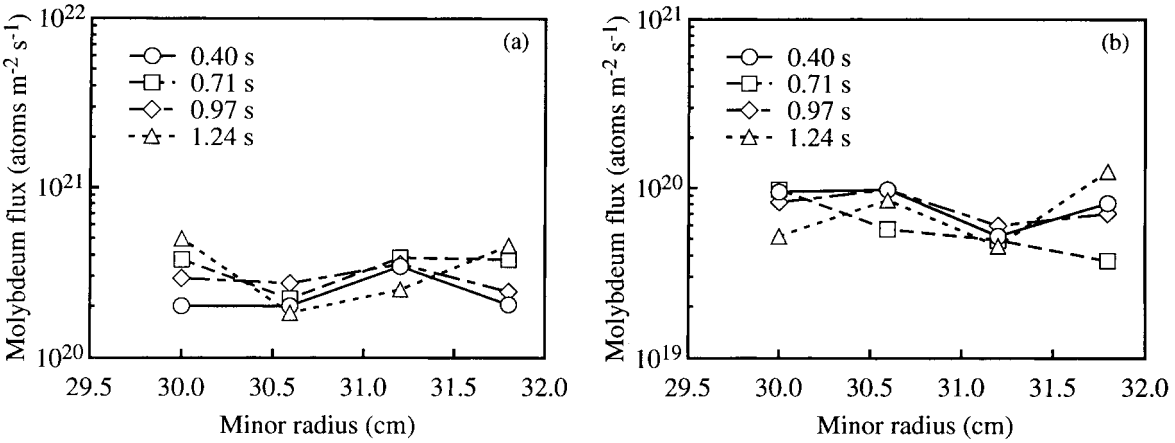

Fig. 3. (a) Radial profile of molybdenum flux at four different times for $\bar{n}_e = 0.8 \times 10^{20}$ m^{-3} plasma discharge for the i$^+$ side of the probe. (b) Radial profile of molybdenum flux at four different times for $\bar{n}_e = 0.8 \times 10^{20}$ m^{-3} plasma discharge for the e$^-$ side of the probe.

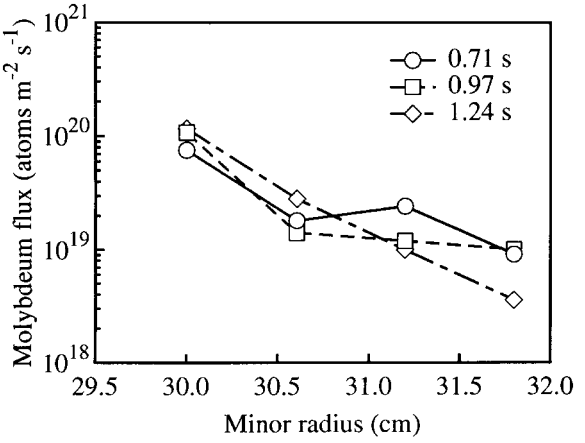

Fig. 4. Radial profile of molybdenum flux at three different times for $\bar{n}_e = 1.3 \times 10^{20}$ m^{-3} plasma discharge for the i$^+$ side of the probe.

the electron density, total particle flux in the SOL: $\Gamma_\perp = (3\text{–}9) \times 10^{21}$ s^{-1}, molybdenum as main impurity ($Z_i = 42$). A cross field flux may be also included in the code for the impurity particles diffusing from the plasma and entering in the SOL, but it has been neglected here because, according to spectroscopic data, it is much lower than the molybdenum flux produced at the limiter and transported along the SOL. In Table 1 we have summarised the comparison between the experimental and simulated data. The total radiation losses have been estimated from the signals provided by an array of bolometric detectors. Langmuir probe measurements have been used to derive the electron temperature and density very close to the probe position for $L_c = 7$ m, while an empirical scaling law [6] has been used to derive the same parameters for $L_c = 2.2$ m.

Here the values of temperature and density are referred to the midplane position. For the case with $L_c = 2.2$ m it has been proven difficult to reproduce satisfactorily the scaled values of T_e with the code using the transport coefficients within their normally assumed range of variation. This may be due to the very short connection length which is quite unusual in FTU. However the temperature value does not seem to affect the result of the code to a large extent.

The impurity flux is calculated from the product of the total ion impurity density at the limiter radius times their velocity, which is assumed to be the same as that of the background ions because of the action of the drag force [7]. In this calculation the total ion density at the probe position has been taken as half the value at the midplane as it is normally assumed for the electron density at the plasma/sheath interface. Quantitatively, the agreement of these fluxes with the experimental data is within a factor 3 for all three cases. The asymmetry between the ion ($L_c = 7$ m) and the electron ($L_c = 2.2$ m) side is satisfactorily well reproduced confirming that the primary effect is related to the different connection length. The predicted value of the impurity flux at the probe, lower at high density than at low density, is in agreement with the experiment. According to the code the main reason for this behaviour is the better screening efficiency of the SOL at high density as well as the lower impurity production rate due to the lower plasma temperature at the limiter plate. As a consequence, the impurity density at the probe location is reduced. The experimental radial profile of the total Mo flux shown in Figs. 3 and 4 can also be reproduced by the code satisfactorily well.

As a comparison the total impurity density radial profiles are shown in Fig. 5 (a) and (b) for $\bar{n}_e = 0.8 \times 10^{20}$ m^{-3} and $\bar{n}_e = 1.3 \times 10^{20}$ m^{-3} respectively, starting from the limiter radius down to the wall position. A high diffusion coefficient $D_\perp = 4$ m^2/s is needed at low density to obtain the quite flat profile, while a substantially lower value $D_\perp = 1$ m^2/s is required to simulate the radial decay at high density. In the model of the SOL the drag force on impurity ions flowing to the limiter decreases radially approaching the wall, mainly due to the reduction of the plasma density. Thus, on the probe we expect a higher probability to detect impurities in the regions close to the wall than in the ones close to the plasma. This physical mechanism, however, is not sufficient to explain the rather flat profile which is reproduced only if a high radial diffusion coefficient is assumed at high density.

Table 1
Comparison between the experimental and simulated data in the SOL for $\bar{n}_e = 1.3 \times 10^{20}$ m^{-3} and $\bar{n}_e = 1.3 \times 10^{20}$ m^{-3}, for the ion and electron connection lengths (7 and 2.2 m, respectively)

	$\bar{n}_e = 0.8 \times 10^{20}$ m^{-3}				$\bar{n}_e = 1.3 \times 10^{20}$ m^{-3}			
	$L_c = 7$ m		$L_c = 2.2$ m		$L_c = 7$ m		$L_c = 2.2$ m	
	Exp.	Code	Exp.	Code	Exp.	Code	Exp.	Code
P_{SOL} (kW)	500	500	500	500	600	600	600	600
n_e ($\times 10^{19}$) m^{-3}	1.1	1.1	0.4	0.4	2.8	2.8	0.9	0.8
T_e (eV)	30	31	15	36	30	22	15	27
Γ_{imp} ($\times 10^{20}$) m^{-2} s^{-1}	3.0	6.0	0.9	1.6	1.0	1.0	–	0.3

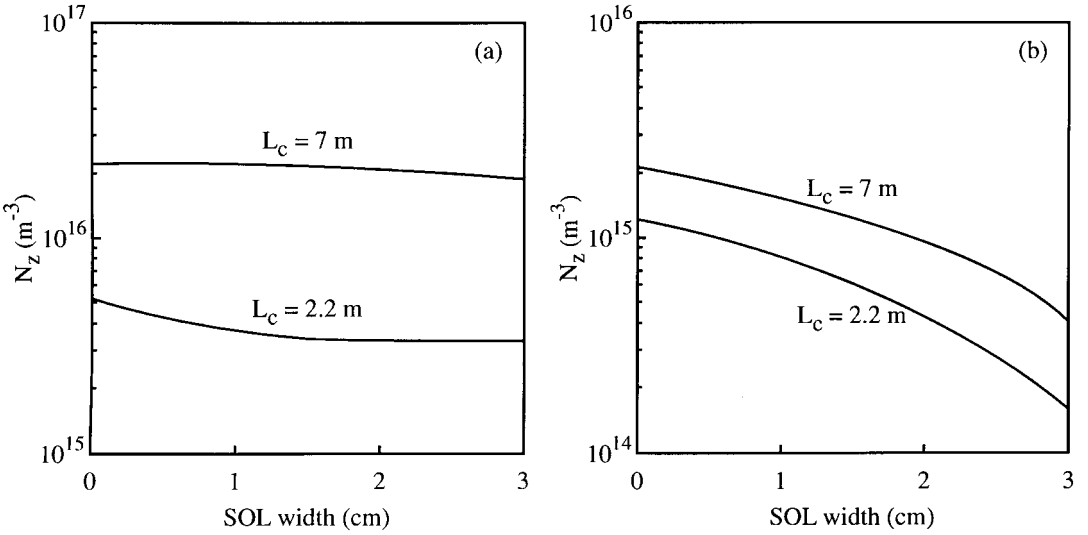

Fig. 5. (a) Total Mo density radial profile for $\bar{n}_e = 0.8 \times 10^{20}$ m^{-3} on the i$^+$ (L_c = 7 m) and e$^-$ (L_c = 2.2 m) side as obtained by the EPIT code. (b) Total Mo density radial profile for $\bar{n}_e = 1.3 \times 10^{20}$ m^{-3} on the i$^+$ (L_c = 7 m) and e$^-$ (L_c = 2.2 m) side as obtained by the EPIT code.

A very interesting point is to relate the experimental results so far illustrated with the value of the impurity density in the central plasma, $n_{Mo}(0)$. The latter is inferred from an absolutely calibrated rotating crystal X-ray spectrometer. $N_{Mo}(0) = 6 \times 10^{16}$ m^{-3} and $n_{Mo}(SOL) = 5 \times 10^{15}$ m^{-3} have been obtained at 0.8×10^{20} m^{-3} while $n_{Mo}(0) = 2 \times 10^{16}$ m^{-3} and $n_{Mo}(SOL) = 2 \times 10^{15}$ m^{-3} have been obtained at 1.3×10^{20} m^{-3}. The ratio $n_{Mo}(0)/n_{Mo}(SOL)$ is about a factor 10 in both cases indicating that the impurity radial profile in the main plasma does not change with density.

Considering a simple transport model with a diffusive term $D_\perp$ plus an inward pinch velocity v_{in} the following relation between $n_{Mo}(0)$ and $n_{Mo}(SOL)$ holds [8]

$$n_{Mo}(0) = n_{Mo}(SOL) \exp\left(\int_0^a dr\, v_{in}/D_\perp\right), \quad (1)$$

where a is the value of the plasma radius. The ratio of $n_{Mo}(0)/n_{Mo}$ (SOL) is a function of $v_{in}/D_\perp$. Therefore its constancy with n_e implies that the impurity transport in the main plasma does not change appreciably with the plasma density. This result is in agreement with previous experimental observations on FTU where differences in the impurity transport have been observed only for plasma discharges with hollow temperature profiles and strong radiation emissivity from the centre [9].

4. Conclusions

Deposition probes have been used for the first time on FTU to measure molybdenum fluxes in the SOL during ohmic plasma discharges. These fluxes have been reproduced satisfactorily well with the 2D multifluid numerical code EPIT which is able to describe the production mechanisms and the dynamics of the impurities in the SOL. The strong asymmetry between the ion and electron side of the probe is mainly related to the different connection lengths with respect to the toroidal limiter. The rather flat profiles observed at low density are reproduced only if the impurity diffusion coefficient is taken sufficiently high, since the impurity retention, which is higher near to the plasma and lower near to the wall, is not sufficient to account for these results.

The ratio between the molybdenum density at the central plasma and that measured in the SOL is about a factor 10 and does not change with density indicating that the impurity transport in the central plasma does not depend on density.

References

[1] M.L. Apicella et al., Nucl. Fusion 37 (1997) 381.
[2] G. Staudenmaier et al., J. Nucl. Mater. 93&94 (1980) 121.
[3] R. Zagórski, J. Tech. Phys. 37 (1) (1996) 7.
[4] R.A. Langely et al., Nucl. Fusion, special issue (1984) 9.
[5] P.C. Stangeby, J. Phys. 18 (1985) 1547.
[6] M. Leigheb, V. Pericoli Ridolfini, R. Zagórski, J. Nucl. Mat. 241&243 (1997) 914.
[7] P.C. Stangeby, J. Phys. D 15 (1982) 1007.
[8] R. Bartiromo et al., Nucl. Fusion 35 (1995) 1161.
[9] L. Gabellieri, G. Mazzitelli, Contr. Fusion Plasma Phys. (Proc. 22nd Eur. Conf. Bournemouth, 1995), vol. 19C, Part I (1995) 77.